Hindawi
International Journal of Aerospace Engineering
Volume 2023, Article ID 3093526, 15 pages
https://doi.org/10.1155/2023/3093526

Research Article

An Intelligent Algorithm for Aerodynamic Parameters Calibration of Wind Tunnel Experiment at a High Angle of Attack

Yeguang Wang,[1,2] **Shitong Jian**,[3] **Zhigang Wang**,[2] **Rui Fan**,[2] **Peng Han**,[2] **and Yongxi Lyu**[3]

[1]*Department of Aeronautics and Astronautics, Fudan University, Shanghai 200433, China*
[2]*Shenyang Aircraft Design and Research Institute of AVIC, Shenyang 110035, China*
[3]*School of Automation, Northwestern Polytechnical University, Xi'an 710072, China*

Correspondence should be addressed to Yongxi Lyu; yongxilyu@nwpu.edu.cn

Received 10 September 2022; Revised 5 December 2022; Accepted 10 December 2022; Published 7 January 2023

Academic Editor: Zhiguang Song

Copyright © 2023 Yeguang Wang et al. This is an open access article distributed under the Creative Commons Attribution License, which permits unrestricted use, distribution, and reproduction in any medium, provided the original work is properly cited.

In this paper, an intelligent algorithm for the aerodynamic parameter calibration of wind tunnel experiments of advanced layout aircraft at a high angle of attack is proposed. The proposed algorithm is based on a homologous comparison and tuning algorithm, and it can effectively improve the accuracy of the wind tunnel experiment model. First, based on the analysis of large oscillation wind tunnel experimental data of an advanced layout scaled aircraft, the high angle of attack wind tunnel experimental model composed of static derivative, dynamic derivative, and rotating balance derivative is established. Second, to improve the accuracy of the wind tunnel experimental model effectively, the idea of combing layered calibration and intelligent algorithm for high angle of attack homologous comparison correction is proposed. The proposed method solves the problems of complex structure, a large amount of data, and poor accuracy in homologous comparison of high angle of attack aerodynamic models of advanced layout aircraft. Finally, the homologous comparison interface software is designed based on MATLAB GUI, which integrates the proposed methods and ideas and realizes effective adjustment of aerodynamic parameters of high angle of attack simulation flight wind tunnel test of an advanced layout aircraft. This study provides a reliable engineering and technical means for subsequent high angle of attack flight test verification of the advanced layout aircraft.

1. Introduction

With the development of computer science and information technology, the aviation industry has stepped into the era of data, and the intelligent technology applied to fighter aerodynamic modeling has developed gradually. The existing aircraft modeling has often been based on wind tunnel test data or computational fluid dynamics (CFD). All static coefficients can be easily obtained, but not all wind tunnels can provide dynamic data. The effects of blocking, scaling, and low Reynolds number reduce the accuracy compared with the full-scale model [1]. These circumstances make flight simulation results based on wind tunnel test data can have a certain deviation from actual flight test data. In addition, at a high angle of attack, this deviation is exacerbated by special gas flow phenomena on the fuselage and wing surfaces. Therefore, it is necessary to modify and verify the aerodynamic model based on wind tunnel data. Tyan et al. [2] used flight data of a small propeller-driven RC airplane to alter the original dynamics model structure, including adjustable gains. The results showed that the output of the adjusted model was close to the flight test data. Liu et al. [3] determined the correction coefficients based on the statistical relationship between the flight test data and simulation data identification results and established the correction coefficient interpolation table based on the law that the correction coefficient changes with the dynamic pressure at different state points. This method did not change the original aerodynamic model. Liu et al. [4] realized the gradual calibration of aerodynamic model data by isolating aerodynamic model parameters with high correlation and obtained the optimal combination of flight test actions and states. Wei et al. [5] proposed the method of checking

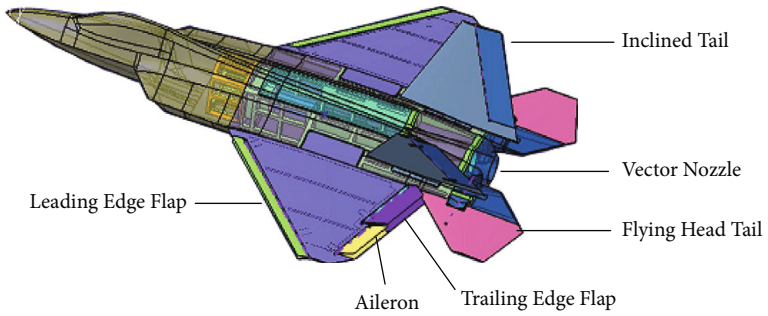

Figure 1: Scale model of the advanced fighter.

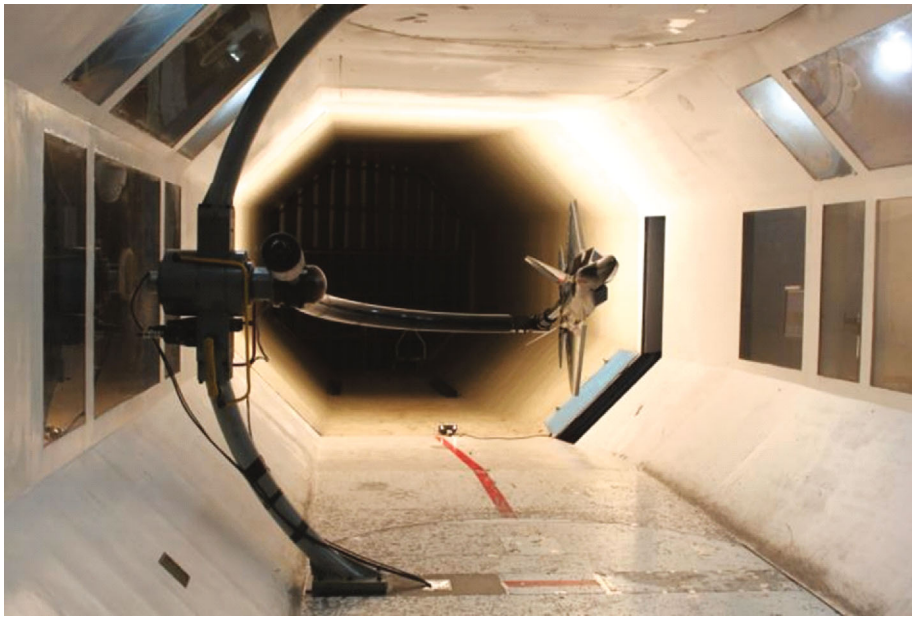

Figure 2: The FL-8 wind tunnel test system photograph.

longitudinal first and then transverse heading and finally dynamic and modified aerodynamic model parameters based on the flight test data and aerodynamic model response. The results showed that the proposed simulation aerodynamic model could meet the standardized tolerance range. Sibilski et al. [6] used indicial functions to identify aerodynamic derivatives of micro airplanes and compared them with derivative source data and could successfully reproduce known phenomena in the dynamics of fighter jets with large head-on angles.

When establishing an aerodynamic database, an important task is to determine a nonlinear model of an aircraft, especially at a high angle of attack, and to ensure its accuracy. However, in the establishment of a nonlinear aerodynamic model with a high angle of attack based on the wind tunnel test data, aircraft aerodynamic force shows characteristics of high nonlinearity, hysteresis, and coupling. Aerodynamic force is no longer a conventional aerodynamic force, and it is also a great challenge to establish an accurate aerodynamic model at high angles of attack. Extensive research on this topic has been conducted worldwide. Goman and Khrabrov [7] believed that a complex, unsteady hysteresis effect of an aircraft at a high angle of attack was caused by vortex bursting. Parameters such as the specific position of vortex bursting were taken as an input of unsteady aerodynamic modeling, and the physical structure of this method was clear. Wang and Cai [8] proposed a differential equation model, which divides the forces and torques of the three axes into static aerodynamic forces, quasi-steady aerodynamic increments, and unsteady aerodynamic increments. In addition, unsteady aerodynamic models such as large oscillation wind tunnel test and model's free oscillation, which can describe unsteady aerodynamic characteristics well, were established. Steck and Rokhsaz [9] applied a neural network to unsteady aerodynamic modeling for the first time and designed a neural network aerodynamic model for delta wings at a high angle of attack of 70°. Gong and Shen [10] used the modeling method of an adaptive neural network model to model unsteady aerodynamics. The results showed that the modeling accuracy of the adaptive neural network model was high, and it could approach unsteady aerodynamics well. Due to the powerful mapping ability, neural networks provide a new method for nonlinear aerodynamic modeling, but they cannot determine an optimal structural model. In contrast,

Table 1: Aerodynamic reference dimensions and mass properties.

Aerodynamic reference	Quantity	Unit
Model scaling ratio	1 : 16	
Weight	8	Kg
Length	1.1825	m
Wingspan	0.8475	m
Wing area	0.3618	m^2
I_{xx}	0.4368	Kg m^2
I_{yy}	0.6595	Kg m^2
I_{zz}	1.0520	Kg m^2
I_{xz}	0.0584	Kg m^2

the existing methods can only determine a comparatively excellent structural model. Chen [11] applied the bifurcation analysis to the behavior analysis of a fixed-wing aircraft with a strake-wing, providing the basic structure of the dynamical system. Nowakowski et al. [12] applied a support vector machine to the unsteady aerodynamic modeling at a high angle of attack. For a small number of samples, the prediction accuracy of this model was much higher compared to the other intelligent learning methods. However, for numerous samples, the calculation was complex, and the cost was high, which could not meet the actual flight requirements.

In this study, a six-degree-of-freedom high angle of attack model with clear physical significance is established based on three components (static, dynamic, and rotating).

Aiming at overcoming the disadvantages of manual gain adjustment, heavy workload, and slow calculation speed when using flight data to calibrate the aerodynamic model, an intelligent optimization algorithm is proposed to correct aerodynamic data with homologous correlation at a high angle of attack. The existing algorithms can be roughly divided into the following groups of population-based algorithms: evolutionary algorithms and swarm intelligence-based algorithms. The genetic algorithm (GA) has been one of the most common evolutionary algorithms. The GA [13] attempts to simulate the genetic and evolutionary process of organisms in nature and belongs to the class of adaptive and globally optimized search algorithms. The differential evolution algorithm [14], like other evolutionary algorithms, operates on the population, but its breeding scheme is different. The immune algorithm [15] is an adaptive algorithm designed by referring to the human immune system that can identify pathogens and is capable of learning, memory, and recognition. The ant colony optimization algorithm [16] is a heuristic random search algorithm that simulates the collective search behavior of ants in nature. The particle swarm optimization algorithm [17] is based on the idea that birds exchange individual information and share flight experiences in the process of predation. This algorithm likens the search space of the optimization problem to the flight space of birds. The solving process of the simulated annealing algorithm [18] is similar to the physical annealing process, and the self-independent variables of the optimization problem are equivalent to the internal energy space of metal and other optimization algorithms.

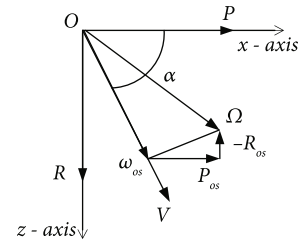

Figure 3: Two-dimensional decomposition of the total angular velocity vector by the first decomposition method.

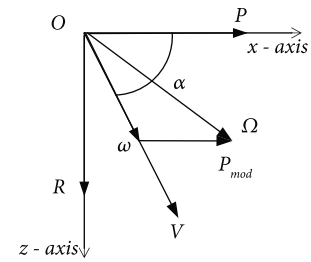

Figure 4: Schematic diagram of the total angular velocity vector decomposition by the second decomposition method.

The main contributions of this study can be summarized as follows:

(1) By locating the causes of errors between the existing wind tunnel test data models and the actual test flight data, the aerodynamic derivatives causing errors are identified by the stratification and progressive method of aerodynamic model parameters

(2) The aerodynamic derivatives are optimized by the intelligent optimization algorithm and transformed into an optimization problem to solve. In this study, the intelligent optimization algorithm is used to modify the aerodynamic database

(3) A set of GUI programs are designed in MATLAB, which can provide necessary guidance and rapid error correction for the aerodynamic database at a high angle of attack

The remainder of this paper is organized as follows. In Section 2, the aircraft model used in this study and the source of wind tunnel data are described. In Section 3, the main process of homologous comparison and the overview of intelligent optimization algorithms are explained. In Section 4, the correction results of aerodynamic data are presented. The main conclusions are given in Section 5.

2. Problem Description

2.1. Wind Tunnel Test. The research object of this study is a scale aircraft model with a typical layout of a fifth-generation aircraft. The three-dimensional effect of the aircraft model is displayed in Figure 1. This model adopts blended wing-body configuration technology to optimize the surface shape. This aircraft has good characteristics under a high angle of attack.

The wind tunnel test data are obtained by an FL-8 wind tunnel test device provided by the AVIC Aerodynamics Research Institute [19]. The scale model of a fighter jet is tested in an FL-8 wind tunnel with two degrees of freedom and a large amplitude oscillation test system. As shown in Figure 2, wind tunnel tests are conducted on the aircraft scaling model. The wind tunnel test device consists of a top and bottom turntable and an aircraft model supporting mechanism. The aerodynamic reference dimensions and mass properties are shown in Table 1.

2.2. Aerodynamic Modeling. Based on the wind tunnel test data, a six-degree-of-freedom nonlinear simulation model of an aircraft is established. The aerodynamics in the body-axis coordinate system are decomposed into static aerodynamics, dynamic oscillating aerodynamics, and circular motion aerodynamics, corresponding to static six-component balance data, forced oscillating balance data, and rotating balance data in wind tunnel test, respectively. However, in the specific process of use, there is an overlap between the forced oscillating balance test and the rotary balance test [20]. Therefore, to build an accurate aerodynamic model, data of the two parts should be properly decomposed to avoid repeated calculation. In general, there are two methods [21] to decompose tail spin motion.

The first decomposition method is to decompose the total angular velocity ω in the process of aircraft movement into λ parallel to the velocity axis and to subtract the oscillation angular velocity P_{os}, Q_{os}, R_{os} corresponding to the rotation component ω_{ss}. Component ω_{ss} is used for the rotary balance test data, and P_{os}, Q_{os}, R_{os} are used for the forced oscillation test data. The total angular velocity is obtained as follows:

$$|\Omega| = \sqrt{P^2 + Q^2 + R^2}. \tag{1}$$

The specific decomposition formula is as follows:

$$\omega_{ss} = (P\cos\alpha + R\sin\alpha)\cos\beta + Q\sin\beta, \tag{2}$$

$$P_{os} = P - \omega_{ss}\cos\alpha\cos\beta, \tag{3}$$

$$Q_{os} = Q - \omega_{ss}\sin\beta, \tag{4}$$

$$R_{os} = R - \omega_{ss}\sin\alpha\cos\beta, \tag{5}$$

where ω_{ss} is the angular velocity component along the velocity axis, and P_{os}, Q_{os}, R_{os} refer to the angular velocity along the body axis.

However, the above method introduces inverse problems. As shown in Figure 3, the total angular velocity is decomposed into three vectors $\omega_{ss}, P_{os}, R_{os}$, but the directions of and are opposite, which affects the accuracy of aerodynamic data.

The second decomposition method is to decompose Ω into ω and P_{mod} along the direction of the velocity vector, as shown in Figure 4, which can solve the inverse problem.

The calculation procedure is to compute ω by Equation (6) setting P_{mod} to zero first. Next, the value of ω is used to obtain Q and R by Equations (7) and (8), respectively. If Q_{mod} and R_{mod} are less than Q and R but have the same sign, then the three components of Ω are $Q_{\mathrm{mod}}, R_{\mathrm{mod}}$, and s; otherwise, the same steps are applied to Equations (7) and (8).

$$P_{\mathrm{mod}} = P - \omega\cos\alpha\cos\beta, \tag{6}$$

$$Q_{\mathrm{mod}} = Q - \omega\sin\beta, \tag{7}$$

$$R_{\mathrm{mod}} = R - \omega\sin\alpha\cos\beta. \tag{8}$$

According to the above calculation procedure, the aerodynamic force and moment coefficients are, respectively, given by:

$$\begin{aligned}
C_x &= C_x(\alpha,\beta) + C_x^{\delta_e}(\alpha)\delta_e + \Delta C_x(\alpha,\beta,\omega_s),\\
C_y &= C_y(\alpha,\beta) + C_y^{\delta_r}(\alpha)\delta_r + C_y^{\delta_a}(\alpha)\delta_a + \Delta C_y(\alpha,\beta,\omega_s),\\
C_z &= C_z(\alpha,\beta) + C_z^{\delta_e}(\alpha)\delta_e + \Delta C_z(\alpha,\beta,\omega_s),\\
C_l &= C_l(\alpha,\beta) + C_l^{\delta_\alpha}(\alpha)\delta_\alpha + C_l^{\delta_r}(\alpha)\delta_r + \frac{c}{2V}\left(C_l^p(\alpha)p + C_l^r(\alpha)r\right) + \Delta C_l(\alpha,\beta,\omega_s),\\
C_m &= C_m(\alpha,\beta) + C_m^{\delta_e}(\alpha)\delta_e + \frac{b}{2V}\left(C_m^q(\alpha)q + C_m^\alpha(\alpha)\alpha\right) + \Delta C_m(\alpha,\beta,\omega_s),\\
C_n &= C_n(\alpha,\beta) + C_n^{\delta_a}(\alpha)\delta_a + C_n^{\delta_r}(\alpha)\delta_r + \frac{c}{2V}\left(C_n^p(\alpha)p + C_n^r(\alpha)r + C_n^\beta(\alpha)\beta\right) + \Delta C_l(\alpha,\beta,\omega_s),
\end{aligned} \tag{9}$$

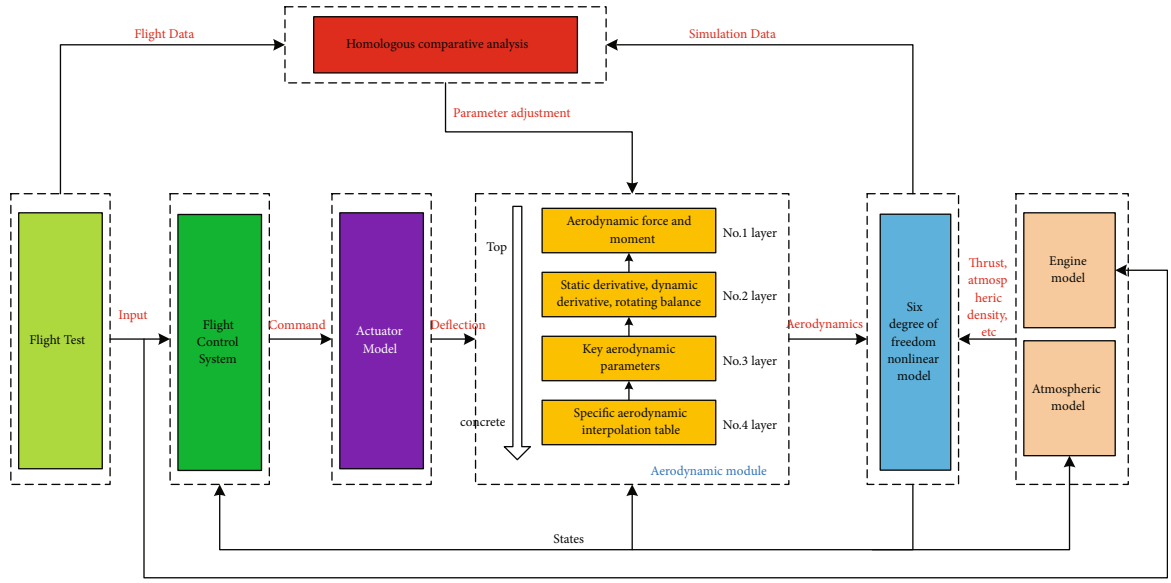

Figure 5: Flowchart of the homologous comparative analysis.

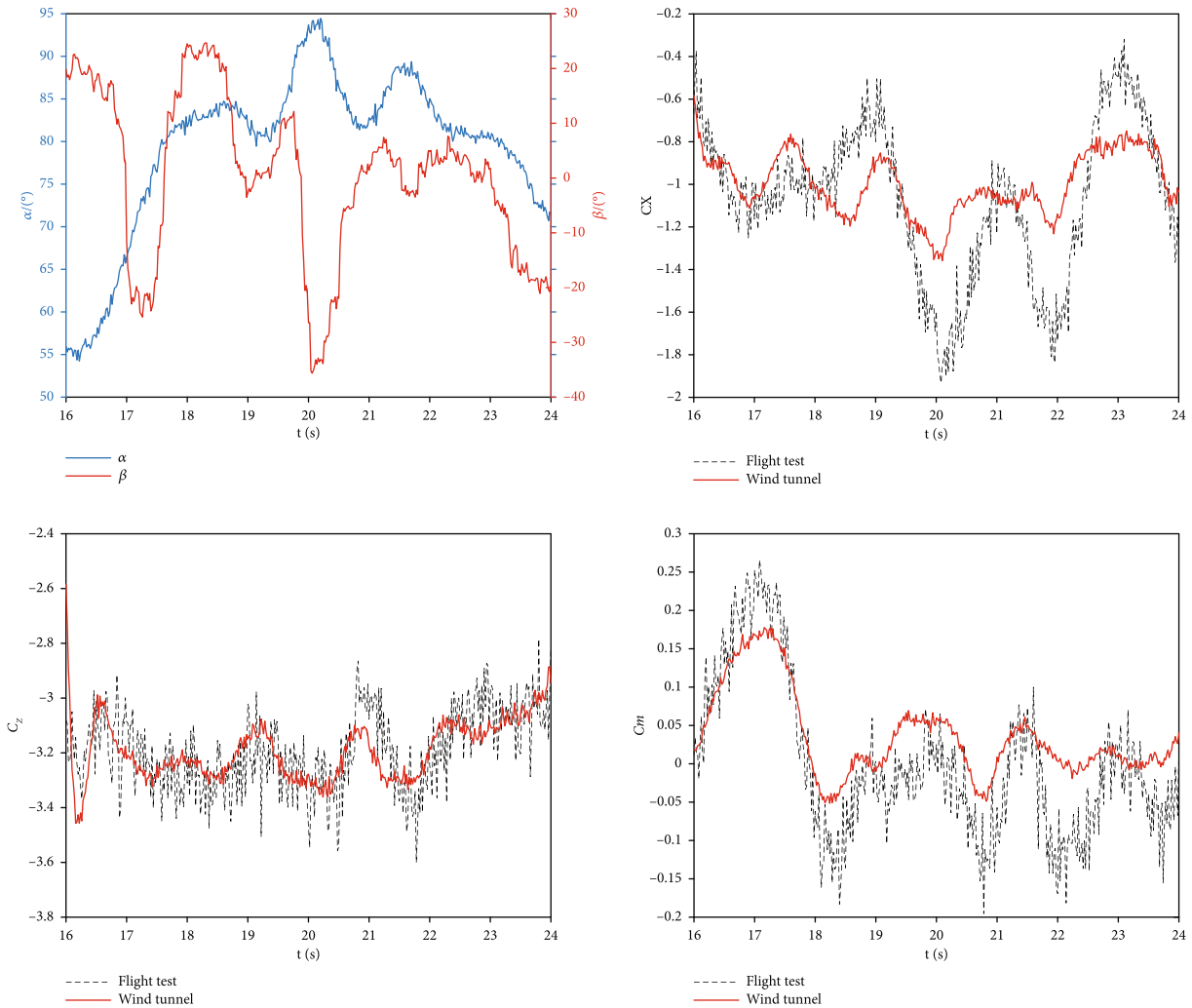

Figure 6: The angles of attack and sideslip measured in the flight test; comparison of the flight data and the wind tunnel modeling data (e.g., C_X, C_Z, and C_m).

The loss function was calculated layer by layer. Then, the module with the smallest loss function was determined, and the next layer was calculated through the module. Aerodynamic parameters were updated according to local and global optimal solutions.

Step 1:

1. Initialize flight state $x_i(0)$ and actuator δ_j
2. For $a = 1, 2, \cdots, n$
3. $k_a = 1 \pm \triangle k$
4. $Err_a = \sum_i \sum_t [x_i(t) - x_i^a(t)]^2$
5. End for
6. $a = \min(Err_a(a))$
7. For $b = 1, 2, \cdots, n_b$
8. $k_{ab} = 1 \pm \triangle k$
9. $Err_b = \sum_i \sum_t [x_i(t) - x_i^b(t)]^2$
10. End for
10. $b = \min(Err_b(b))$
11. For $a = 1, 2, \cdots, n$
12. $k_{abc} = 1 \pm \triangle k$
13. $Err_c = \sum_i \sum_t [x_i(t) - x_i^c(t)]^2$
14. End for
15. For $d = 1, 2, \cdots, n_c$
16. $k_{abcd} = 1 \pm \triangle k$
17. $Err_d = \sum_i \sum_t [x_i(t) - x_i^d(t)]^2$
18. End for
19. $d = \min(Err_d(d))$

Step 2:

1: While not stop
2: For $i = 1, 2, \cdots, N$
3: Update the optimization algorithm parameters
4: $C_{abcd}(\alpha, \beta, \delta, \cdots) = opt$
5: If $fit(C_{abcd}) < fit(pBest)$
6: $pBesti = C_{abcd}$;
7: If $fit(pBesti) < fit(gBest)$
8: $gBest = pBesti$
9: End for
10: End while

Step 3:

1: For $i = 1, 2, \cdots, M$
2: If $Err(gBest) < Err(C_{bm}) * F$
3: $C_{abcd} = gBest$
4: Else go to step 2
5: End if
6: End for

Algorithm 1: The main process the homology comparison.

where V is the space velocity; α and β are the angle of attack and angle of sideslip, respectively; δ_e, δ_a and δ_r are the angle of the elevator, angle of aileron, and angle of rudder, respectively.

3. Homologous Contrastive Process

3.1. Homologous Comparative Analysis Flowchart. The relationship between the flight test data and simulation data and the parameter adjustment ideas and levels in the proposed model are shown in Figure 5. The lever command in the flight test data is input to the control system and engine model through solution, and the control system outputs the solution command to the steering gear model. Next, the steering gear model obtains the rudder deviation and sends it to the aerodynamic solution module. In the aerodynamic solution module, parameter adjustment is the key parameter. The thrust, atmospheric density obtained by the engine model and atmospheric model and the aerodynamic force obtained by the aerodynamic solution module are input into the six-degree-of-freedom nonlinear mathematical model of an aircraft. The simulation data are obtained and analyzed using the flight test data. The simulation analysis error is compared with the evaluation criterion of homologous comparison, which can guide the parameter adjustment.

3.2. Calibration Method. After the unsteady aerodynamic model of an aircraft is designed using the above-presented procedure, the accuracy of the model has to be verified and modified if needed. In view of correction, the homologous contrast correction method is used. Homologous contrast calibration of an aerodynamic model refers to the usage of

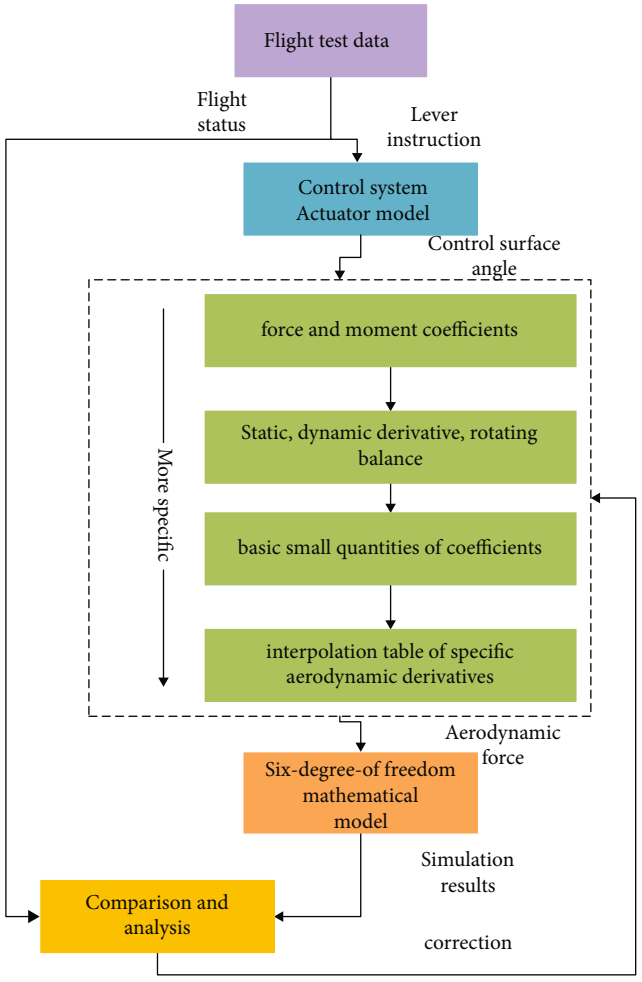

Figure 7: Flowchart and data direction of the homology comparison method and modeling; green boxes indicate the aerodynamic data hierarchy.

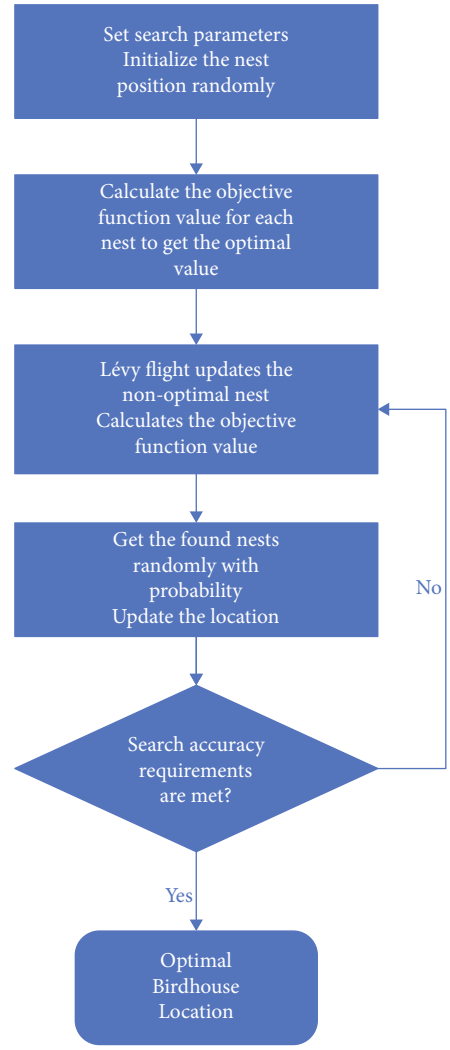

Figure 8: The flowchart of the CS algorithm.

flight test data of an actual aircraft to modify the aircraft aerodynamic model based on the wind tunnel test data so that the deviation between the modified aircraft aerodynamic model's output data and the actual flight test data under the same state can meet the tolerance guidelines [22] specified by the FAA/JAR (joint aviation requirements). Flight measurements with these tolerances define a range within which the model response must meet specified accuracy requirements.

The experimental data used in this study were real flight data of a scaled-down model of a fighter jet. The data were collected when the aircraft performed dynamic maneuvers at a high angle of attack in the air, and the time course was recorded for 80 s with a sampling time of 20 ms. We chose the representative 8 s flight data, that is, the process of increasing the angle of attack, to carry out the identification and verification work in this paper. The flight data were checked for consistency, and the flight path was reconstructed. The aerodynamic response historical data were obtained from the flight state data. The angles of attack and sideslip measured in the flight test are shown in Figure 6.

As shown in Figure 6, there were large deviations in the angle of attack, angle of sideslip, force coefficients of the x- and z-axis, and pitching moment coefficients between the data obtained by the data-based aerodynamic wind tunnel model and the test flight data under the same conditions. This was because the wind tunnel tests did not fully match the flight conditions, especially when the aircraft had a high angle of attack. It should be noted that if a deviation of any of the three parameters is too large, it is necessary to modify the aerodynamic model parameters established using the wind tunnel data. To modify the aerodynamic model according to the deviations, the aerodynamic derivative causing the deviation should be determined first. A method for locating the aerodynamic derivative is proposed in this study. According to the structure and mathematical relationship of the aerodynamic model, aerodynamic data can be divided into four levels: force and moment coefficients, static dynamic derivative rotating balance, basic small quantities of coefficients, and interpolation table of specific aerodynamic derivatives. The aerodynamic model's correction coefficient is defined so that the actual output of the aerodynamic module is equal to the

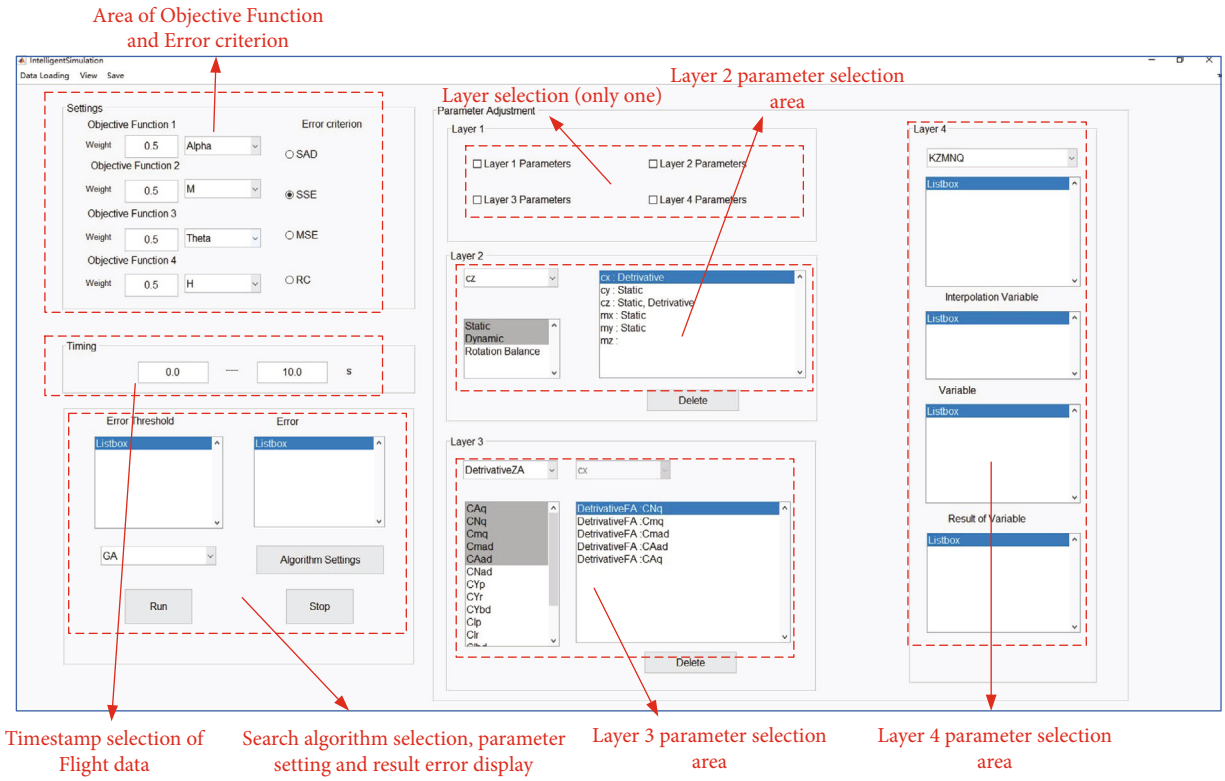

Figure 9: The illustration of the interface of the developed homology comparison intelligent optimization software.

original output multiplied by the correction coefficient. The change in the state response caused by changing the correction coefficient at each level is analyzed, and the module with the most significant response change is taken as an aerodynamic module causing the deviation. The specific aerodynamic derivative interpolation table is obtained layer by layer.

The main steps of the homology comparison process are as follows. In Step 1, according to the above-mentioned types of stratification of aerodynamic data, the loss function is calculated in each layer one by one, and then the module with the smallest loss function is determined, and the next layer is calculated, repeating up to the fourth layer: the specific aerodynamic data interpolation table. In Step 2, the parameters of the intelligent optimization algorithm are gradually updated to calculate the current fitness function and to determine the globally optimal solution. In Step 3, the algorithm stops if the required accuracy is satisfied and returns to Step 2; otherwise, it adjusts the optimization-seeking parameter settings. The main process the homology comparison algorithms are shown in Algorithm 1.

The flowchart of the homologous comparison method is presented in Figure 7. As shown in Figure 7, first, the flight status parameters and stick instructions in the test flight data [23] are separated. The stick instructions are input into the control system and rudder actuator model in the simulation model. The corresponding rudder deflection is fed to the aerodynamic model, and simulation results are obtained by the six-degree-of-freedom mathematical model. Then, the results are compared with the actual flight test data to obtain the deviation and influence. Accordingly, the aerodynamic parameters are modified. Finally, the modified aerodynamic parameters are verified, and the modified effects are analyzed.

When the aerodynamic model is modified, the specific strategy is to take the specific aerodynamic derivative or the aerodynamic model correction coefficient as an optimization variable of the intelligent optimization algorithm. The deviation between the aerodynamic model's state response and actual flight test data is regarded as an objective or fitness function, and an optimization algorithm is used to modify the aerodynamic model parameters. If the aerodynamic derivative is used as an optimization variable, the aerodynamic model parameters will be changed. In contrast, if the correction coefficient is taken as an optimization variable, the cause of the deviation will be determined more accurately, and the aerodynamic model will not change.

When calculating the deviation between the aerodynamic model response and actual flight test data, different aerodynamic derivatives require using different calculation methods. When the pitching moment coefficient is corrected longitudinally, the considered parameters include the angle of attack, rate of pitch, and pitch angle. When the rolling torque coefficient is corrected laterally, the roll angle and rate of the roll are concerned. The longitudinal loss function is defined as follows:

$$Er = k_\alpha \cdot \sum_i^n (\alpha_0(i) - \alpha(i))^2 + k_\theta \cdot \sum_i^n (\theta_0(i) - \theta(i))^2 + k_q \cdot \sum_i^n (q_0(i) - q(i))^2, \tag{10}$$

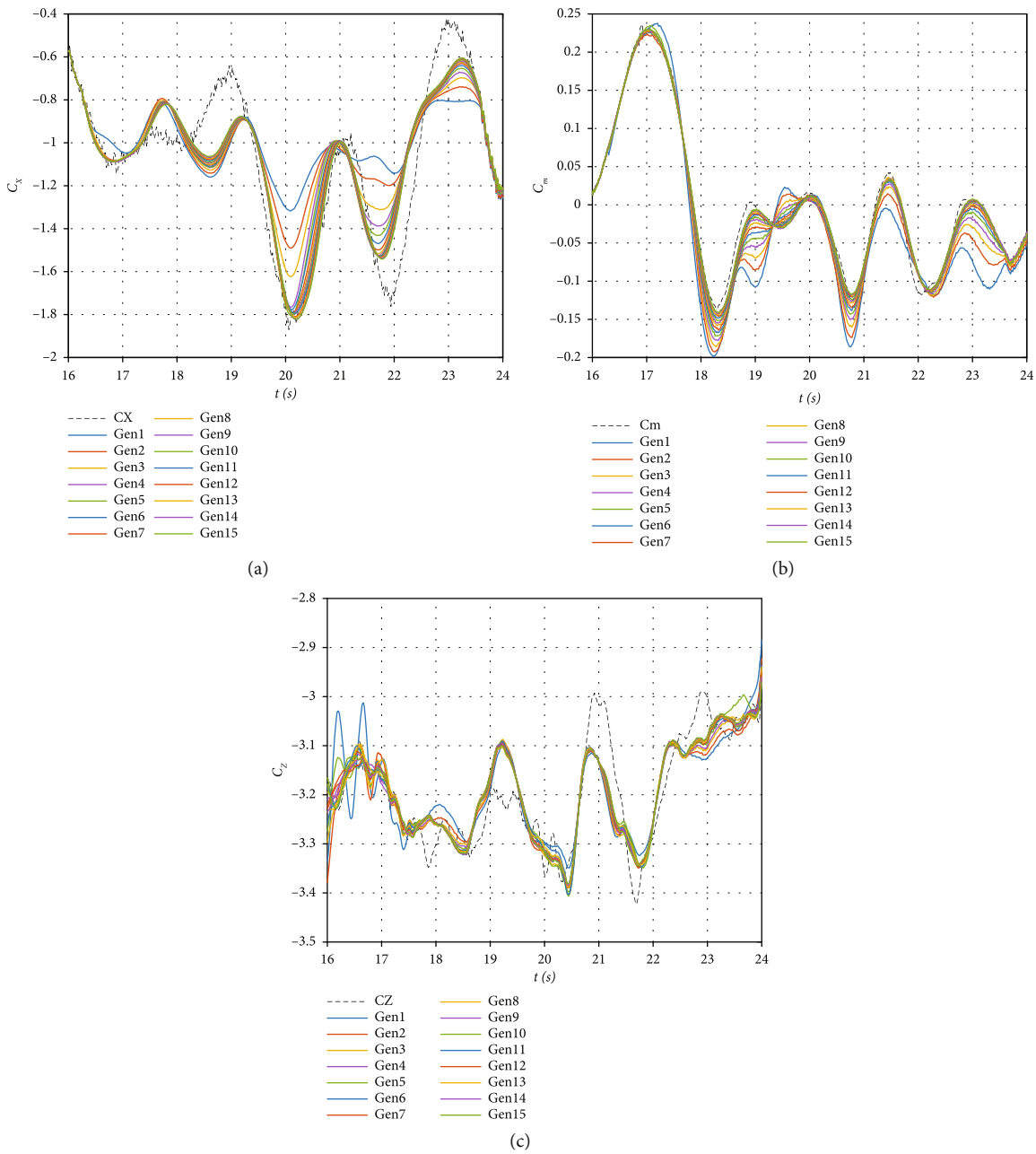

Figure 10: Results of the NSGA-II generation by generation: (a) C_X, (b) C_m, and (c) C_Z.

where k_α, k_θ, and k_q denote the coefficient factors, which can be adjusted according to the size, relationship, and weight of the three variables.

3.3. Homologous Contrastive Mathematical Methods. In the modification of specific aerodynamic derivatives, the popular multiobjective optimization methods can be used to find the best equilibrium solution for the calculation parameters of a model within the range of given aerodynamic derivatives. It should be noted that multiobjective optimization problems do not have an optimal solution, and all possible solutions are called noninferior solutions, i.e., Pareto solutions. Multiobjective optimization algorithms can be roughly divided into traditional optimization algorithms and intelligent optimization algorithms. The traditional methods include linear programming [24] and nonlinear programming, while intelligent optimization algorithms [25] mainly include the GA, particle swarm optimization algorithm, simulated annealing algorithm, and ant colony optimization algorithm. Among the intelligent optimization algorithms, the most popular is the NSGA-II algorithm, which has become one of the benchmark algorithms in the intelligent optimization field because of its advantages of being simple and effective and obvious comparative advantages.

The NSGA algorithm is a multiobjective GA based on the Pareto optimal solution, which introduces a nondominated classification algorithm and simplifies a multiobjective function to a single fitness function. The main advantage of this algorithm is that noninferior optimal solutions are evenly

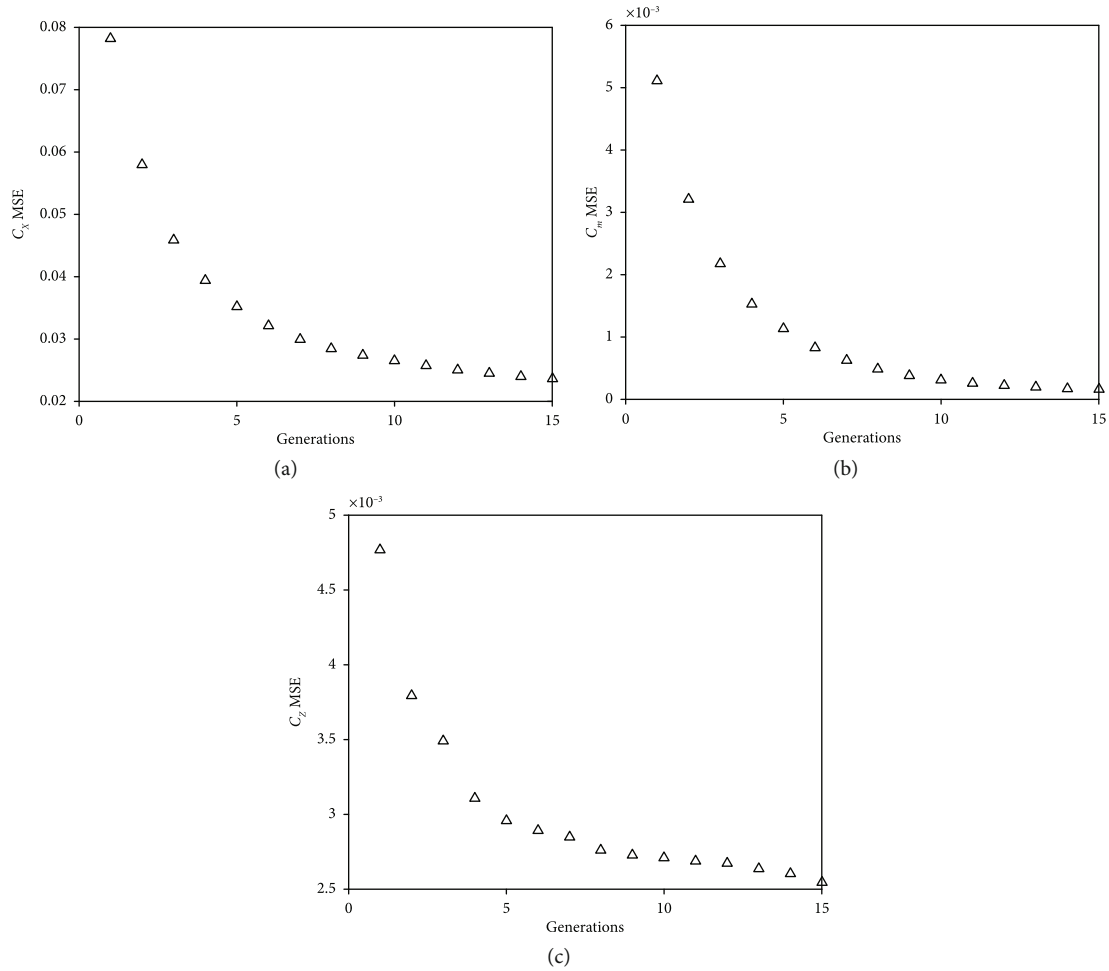

Figure 11: Mean square error of NSGA-II generation by generation: (a) C_X, (b) C_m, and (c) C_Z.

distributed, allowing the existence of multiple different equivalent solutions [26]. Its disadvantages are high computational complexity and lack of elite strategy [27]. In view of these shortcomings, Deb et al. [28] proposed the NSGA-II algorithm, which reduces the computational complexity by introducing the fast nondominated sorting algorithm and elite strategy, and adopting the crowding and crowding comparison operator. In this way, the computational complexity of the algorithm can be reduced without the need to specify the sharing parameter δ_{share}. The individuals in the Pareto optimal solution frontier can be evenly extended to the whole Pareto domain, and the diversity of the population can be guaranteed.

The specific steps of applying the NSGA-II algorithm to the aerodynamic model established by wind tunnel test data are as follows:

(1) Establish the mapping between the individual population and aerodynamic model in the NSGA-II algorithm. After determining the aerodynamic derivative causing the deviation, each individual dimension in the population corresponds to a value in the interpolation table of the specific aerodynamic derivative in the positional aerodynamic derivative term

(2) The calculation error between the aerodynamic model data and the flight test data is used as a fitness function of the NSGA-II algorithm to minimize the error, namely, to perform multiobjective optimization

In addition, the cuckoo search (CS) algorithm [29] is another emerging swarm intelligence optimization algorithm. This algorithm simulates the cuckoo's nesting breeding behavior and Lévy flight mechanism and can obtain an optimal solution quickly and effectively. In essence, the Lévy flight [30] is a random walk process, which includes small high-frequency step and long low-frequency step. The long step is conducive to global search, while the small step is conducive to the local search, thus improving the search accuracy.

The flowchart of the CS algorithm is shown in Figure 8.

4. Simulation Results

In this study, based on the GUI toolbox of MATLAB, the homology comparison correction and analysis software of high angle of attack is designed. The main functions include the import and modification of test flight data, the selection

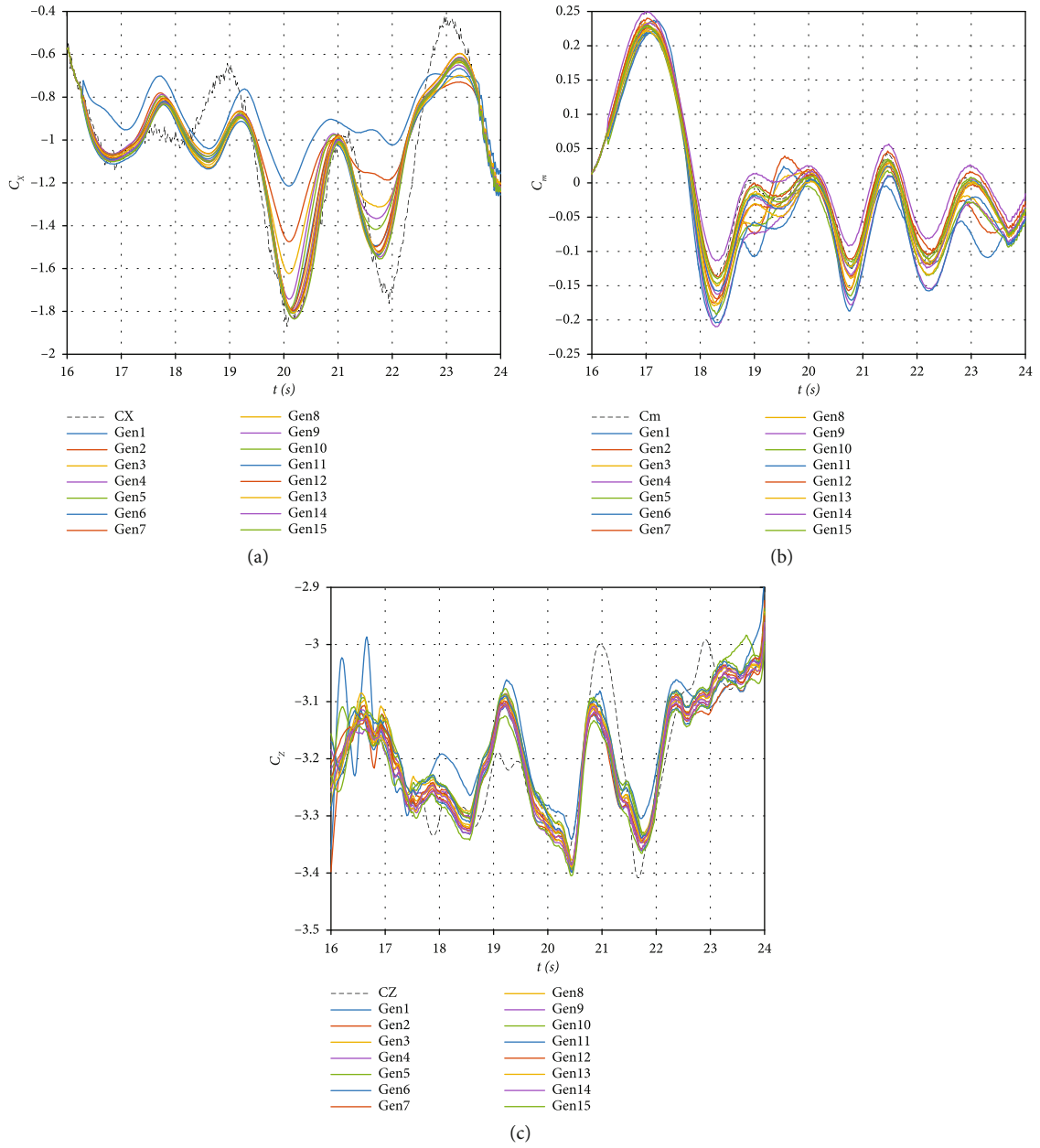

Figure 12: The CS results: (a) C_X, (b) C_m, and (c) C_Z.

of objective function of intelligent optimization algorithm, the selection of error evaluation criteria, the start and end times of simulation (compared with the test flight data), the selection of intelligent optimization algorithm, the configuration of optimization algorithm, and the selection and adjustment of parameters of four layers of the aerodynamic model. The simulation interface is shown in Figure 9.

The evaluation criteria are as follows:

(1) Error sum:

$$z = \sum [\omega_1 (\mathbf{x}_1 - \widehat{\mathbf{x}}_1) + \omega_2 (\mathbf{x}_2 - \widehat{\mathbf{x}}_2) + \cdots + \omega_n (\mathbf{x}_n - \widehat{\mathbf{x}}_n)]. \quad (11)$$

(2) Sum of squares of errors:

$$z = \sum \left[\omega_1 (\mathbf{x}_1 - \widehat{\mathbf{x}}_1)^2 + \omega_2 (\mathbf{x}_2 - \widehat{\mathbf{x}}_2)^2 + \cdots + \omega_n (\mathbf{x}_n - \widehat{\mathbf{x}}_n)^2\right]. \quad (12)$$

(3) Sum of mean square error:

$$z = \sqrt{\sum \left[\omega_1 (\mathbf{x}_1 - \widehat{\mathbf{x}}_1)^2 + \omega_2 (\mathbf{x}_2 - \widehat{\mathbf{x}}_2)^2 + \cdots + \omega_n (\mathbf{x}_n - \widehat{\mathbf{x}}_n)^2\right]}. \quad (13)$$

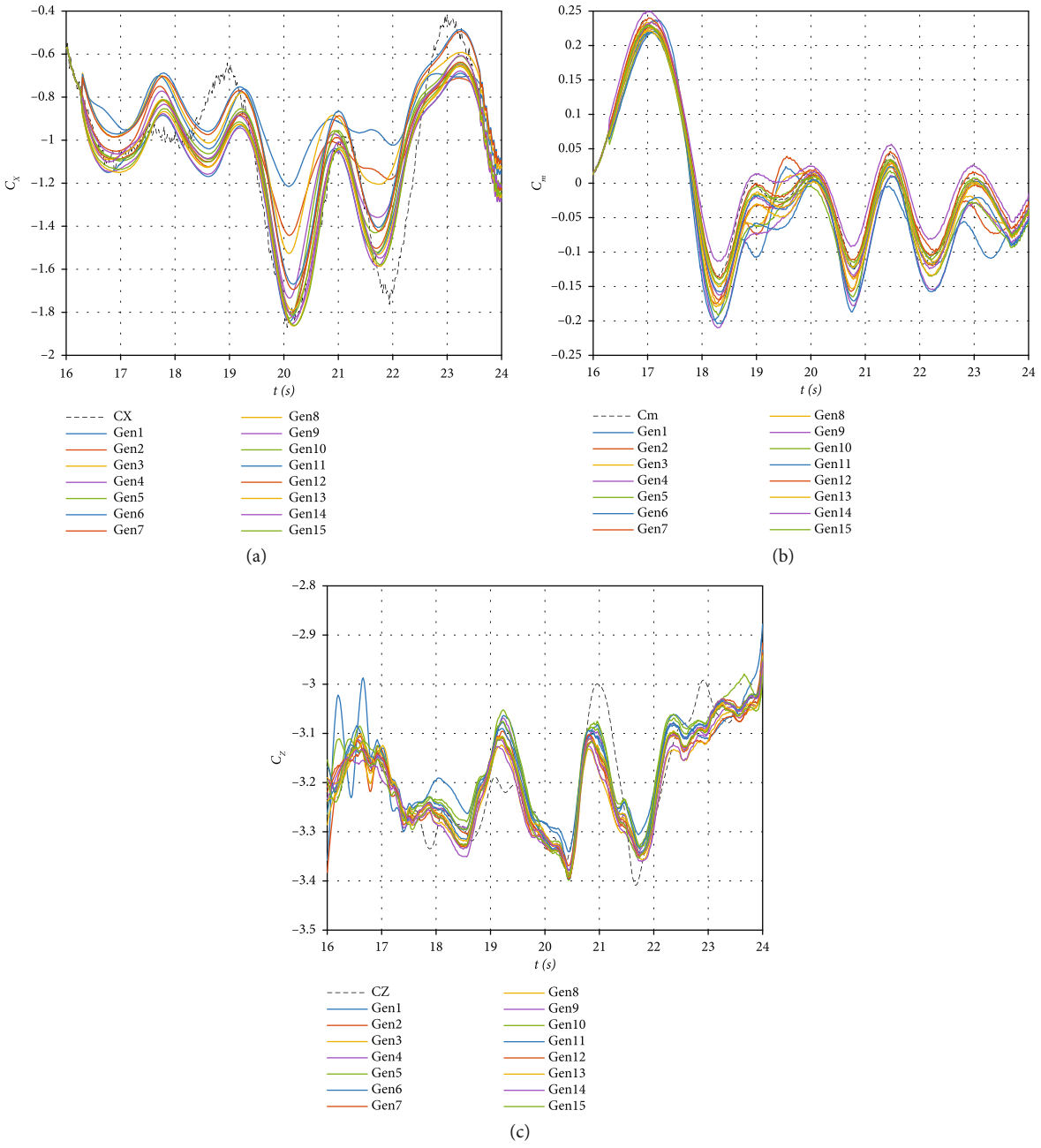

Figure 13: The GA results: (a) C_X, (b) C_m, and (c) C_Z.

(4) Correlation coefficient:

$$z = \sum [\omega_1 r_1 + \omega_2 r_2 + \cdots + \omega_n r_n], r_i = \frac{\sum \mathbf{x}_i \hat{\mathbf{x}}_i - \sum \mathbf{x}_i \sum \hat{\mathbf{x}}_i / N}{\sqrt{\left(\sum \mathbf{x}_i^2 - (\sum \mathbf{x}_i)^2 / N\right)\left(\sum \hat{\mathbf{x}}_i^2 - (\sum \hat{\mathbf{x}}_i)^2 / N\right)}}, \quad (14)$$

where the key state parameters in the flight test data are $x_1, x_2, \cdots, x_n$, the corresponding key state parameters obtained by digital simulation are $\hat{x}_1, \hat{x}_2, \cdots, \hat{x}_n$, and the weighted values of the evaluation standard of different flight state information are $\omega_1, \omega_2, \cdots, \omega_n$, respectively.

After loading the simulated flight test data, the objective function, error criterion, start-stop time, optimization algorithm, and several aerodynamic parameters of a certain layer were selected to start the simulation. According to the simulation result curve and data error, the aerodynamic parameters were manually modified to obtain a more general optimal solution.

Namely, to modify aerodynamic model parameters, the model output data were compared with the test flight data. For instance, for the longitudinal movement of an aircraft, C_X, C_Z, and C_m were taken as optimization objects, and the simulation optimization program was run once. The simulation results obtained by the NSGA-II optimization algorithms are shown in Figure 10. In this case, all aerodynamic parameters

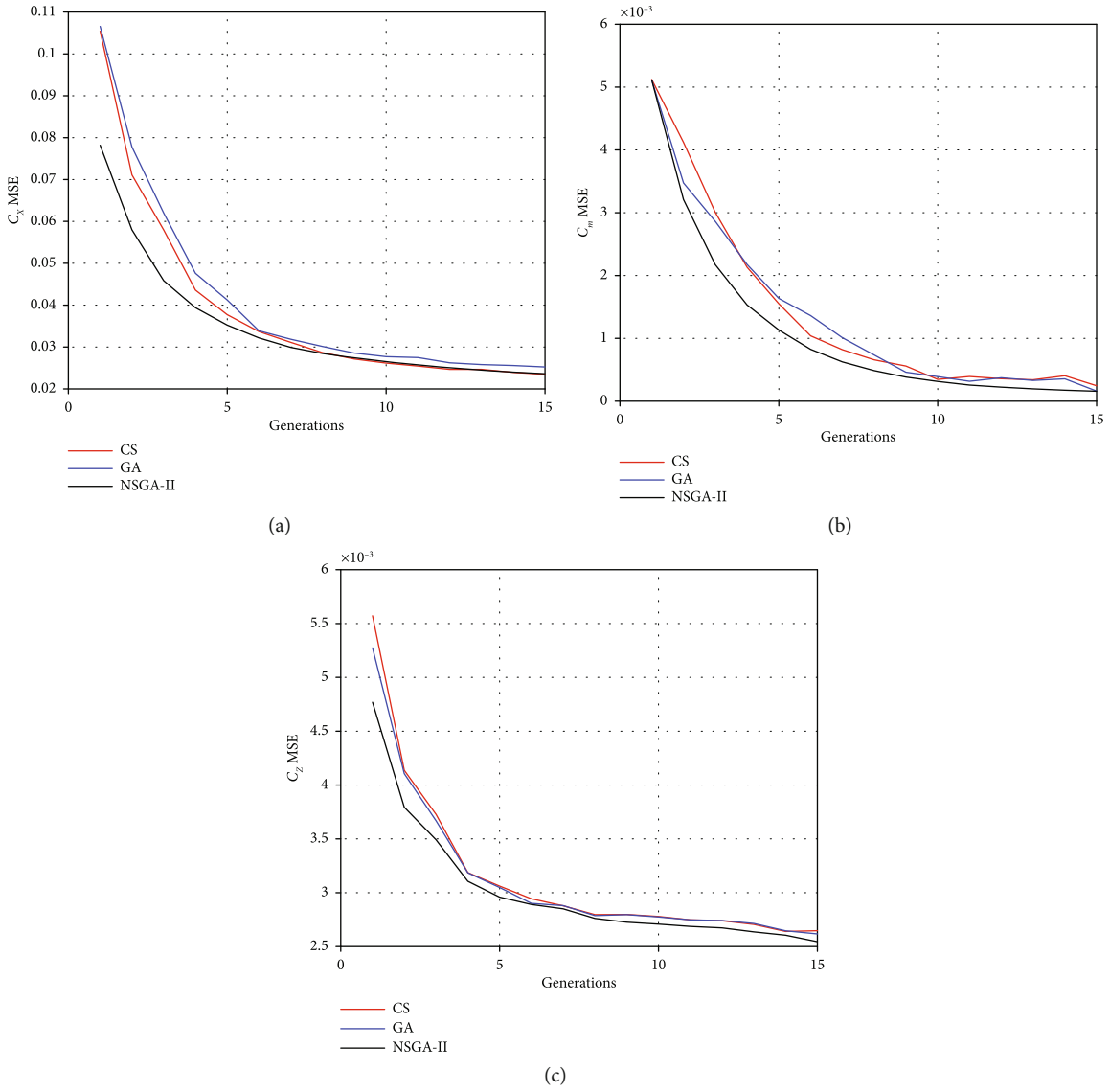

Figure 14: The MSE change with the number of generations: (a) C_X, (b) C_m, and (c) C_Z.

Table 2: The MSE results of different methods.

Correction algorithm	Wind tunnel data			Model correction data		
	C_X	C_m	C_Z	C_X	C_m	C_Z
GA	0.1167	0.0062	0.0073	0.0252	0.000245	0.00262
CS	0.1167	0.0062	0.0073	0.0246	0.000160	0.00265
NSGA-II	0.1167	0.0062	0.0073	0.0236	0.000158	0.00255

of C_X and C_m were processed sequentially by the optimization algorithm under the same settings, which is called one generation of optimization seeking. The results after each generation were gradually approximating the flight data based on the wind tunnel model. Figure 11 shows the mean square error results of the aerodynamic forces and moments after each iteration.

The corrections of the force coefficients on the x-axis were taken as a cause to demonstrate the correction process of a homologous comparison. On the basis of more accurate static coefficients, the results of three different optimization algorithms are presented in Figures 12–14. Figures 12 and 13 show the optimization results of the CS and GA under the same simulation conditions. Figure 14 illustrates variations in the mean square error with the number of simulation generations for the three different methods. During the iterative process, the convergence rate of the three algorithms differed, but eventually, they all converged to a better range than wind tunnel modeling data. Since the angle of attack in the simulation was between 50° and 90°, the corresponding modified aerodynamic derivative interpolation table was within the same range. The interpolation table data and optimization results that were beyond this range were considered not accurate enough.

The comparison of the root mean square error of the prediction results of the above three methods is shown in

Table 2. The results of the correction of the flight data of the scaled-down model of the real fighter aircraft under a high angle of attack showed that the homologous comparison correction method could achieve good correction of the aircraft aerodynamic data. The data correction model based on the intelligent search algorithm could effectively reduce the difference between digital simulation data with the wind tunnel data model and the real aircraft flight data; the average error was reduced to 74% of the mean square error. In addition, the reconfiguration and modeling of the flight test data achieved good noise immunity and robustness in practical engineering applications.

5. Conclusions

In this paper, an intelligent optimization algorithm is applied to the calibration and correction of the aircraft aerodynamic model, and a homologous comparison method of the flight test data is proposed. After the in-depth layer-by-layer analysis, the aerodynamic derivative terms causing the model state response deviation are determined. The state-of-the-art intelligent optimization algorithms are used to modify the aerodynamic derivative interpolation table and to verify the performances of the proposed method. The results show that the accuracy of the modified aerodynamic model is significantly improved, and its model response is closer to the flight test data compared to the other algorithms. Therefore, the proposed homologous comparison method based on an intelligent optimization algorithm can correct the aerodynamic model parameters accurately and comprehensively, which plays an important role in the aircraft model calibration.

However, when the intelligent optimization algorithm is applied to the aircraft aerodynamic model, due to a large amount of data, the optimization process is slow. In addition, in the proposed complex mathematical model, the convergence and stability of the intelligent optimization algorithm have not been proven by mathematical theory. In the future, a combination of the aircraft aerodynamic model and intelligent optimization algorithm could be used to improve the calculation speed of the proposed method while meeting the requirements for correction accuracy. Also, the model convergence and stability could be verified and analyzed while improving the algorithm.

Data Availability

This paper involves the data of model aircraft, and the specific data can be seen in the aircraft description section of the paper.

Conflicts of Interest

The authors declare no conflict of interest.

Authors' Contributions

Y.W. conceived the research idea. S.J. and R.F. developed the theory and performed the computations. S.J., R.F., and P.H. verified the analytical methods. Y.L. and Z.W. supervised the findings of this work. All authors discussed the results and contributed to the final manuscript.

Acknowledgments

The authors would like to thank the AVIC Aerodynamics Research Institute for providing valuable wind tunnel test data through the project cooperation. This work was supported by the National Natural Science Foundation of China (Grant No. 62173277), Natural Science Foundation of Shaanxi Province (2022JM-011), and Shaanxi Province Key Laboratory of Flight Control and Simulation Technology.

References

[1] A. Kamal, A. M. Aly, and A. Elshabka, "Tuning of airplane flight dynamic model using flight testing," in *AIAA Modeling and Simulation Technologies Conference*, p. 1595, Kissimmee, Florida, 2015.

[2] M. Tyan, M. Kim, V. Pham, C. K. Choi, T. L. Nguyen, and J.-W. Lee, "Development of advanced aerodynamic data fusion techniques for flight simulation database construction," in *2018 Modeling and Simulation Technologies Conference*, p. 3581, Atlanta, Georgia, 2018.

[3] Q. Liu, Y. H. Liu, and W. S. Zhang, "Simulator aerodynamic model calibration method based on the flight test," *Flight Dynamics*, vol. 33, no. 3, pp. 265–268, 2015.

[4] Y. H. Liu, Q. Liu, and Y. F. Zhang, "Calibration and verification flight test method for the aerodynamics model of FBW transport category aircraft," *Flight Dynamics*, vol. 36, no. 3, pp. 80–83+88, 2018.

[5] Y. Wei, D. C. Zhang, B. M. Zhao et al., "Flight simulator aerodynamic model calibration based on flight test data," *Flight Dynamics*, vol. 35, no. 1, pp. 84–88, 2017.

[6] K. Sibilski, M. Nowakowski, D. Rykaczewski et al., "Identification of fixed-wing micro aerial vehicle aerodynamic derivatives from dynamic water tunnel tests," *Aerospace*, vol. 7, no. 8, p. 116, 2020.

[7] M. Goman and A. Khrabrov, "State-space representation of aerodynamic characteristics of an aircraft at high angles of attack," *Journal of Aircraft*, vol. 31, no. 5, pp. 1109–1115, 1994.

[8] Q. Wang and J. Cai, "Unsteady aerodynamic modeling and identification of airplane at high angles of attack," *Acta Aeronautica et Astronautica Sinica-Series A and B-*, vol. 17, pp. 391–398, 1996.

[9] K. Rokhsaz and J. E. Steck, "Use of neural networks in control of high-alpha maneuvers," *Journal of Guidance, Control, and Dynamics*, vol. 16, no. 5, pp. 934–939, 1993.

[10] Z. Gong and H. Shen, "Structure self-adapting ANN method in modeling of unsteady aerodynamics," *Flight Dynamics-XIAN-*, vol. 25, no. 4, p. 13, 2007.

[11] Y. Chen, "Modeling of longitudinal unsteady aerodynamics at high angle-of-attack based on support vector machines," in *2012 8th international conference on natural computation*, pp. 431–435, Chongqing, China, 2012.

[12] M. Nowakowski, K. Sibilski, A. Sibilska-Mroziewicz, and A. Żyluk, "Bifurcation flight dynamic analysis of a strake-wing micro aerial vehicle," *Applied Sciences*, vol. 11, no. 4, p. 1524, 2021.

[13] J. Genlin, "Survey on genetic algorithm," *Computer Applications and Software*, vol. 2, no. 1, pp. 69–73, 2004.

[14] K. Price, R. M. Storn, and J. A. Lampinen, *Differential Evolution: A Practical Approach to Global Optimization*, Springer Science & Business Media, 2006.

[15] A. Watkins, J. Timmis, and L. Boggess, "Artificial immune recognition system (AIRS): an immune-inspired supervised learning algorithm," *Genetic Programming and Evolvable Machines*, vol. 5, no. 3, pp. 291–317, 2004.

[16] M. Dorigo and C. Blum, "Ant colony optimization theory: a survey," *Theoretical Computer Science*, vol. 344, no. 2-3, pp. 243–278, 2005.

[17] J. Kennedy and R. Eberhart, "Particle swarm optimization," in *Proceedings of ICNN'95-international conference on neural networks*, vol. 4, pp. 1942–1948, 1995.

[18] P. Bangert, *Optimization: Simulated Annealing*, Springer Berlin Heidelberg, 2012.

[19] C. Liu, Z. Zhao, and C. Bu, "Double degree-of-freedom large amplitude motion test technology in low speed wind tunnel," *Acta Aeronautica et Astronautica Sinica*, vol. 37, no. 8, pp. 2417–2425, 2016.

[20] R. Qiulei and H. Yixin, "High angle of attack aerodynamic modeling and simulation and analysis of stall/spin mode," *Chinese Journal of Applied Mechanics*, vol. 35, no. 3, pp. 472–478, 2018.

[21] J. Kalviste, "Use of rotary balance and forced oscillation test data in six degrees of freedom simulation," in *9th Atmospheric Flight Mechanics Conference*, p. 1364, San Diego,CA,U.S.A, 1982.

[22] FAA A C, *Airplane Simulator Qualification (AC 120–40B)*, Federal Aviation Administration (FAA), Washington, DC, 1991.

[23] L. Chao, Q. Liu, and F. Tian, "Research on flight test data processing method applied to the identification of aerodynamic derivatives," *Advances in Aeronautical Science and Engineering*, vol. 5, no. 2, pp. 187–192, 2014.

[24] A. Abur and M. Kezunovic, "A simulation and testing laboratory for addressing power quality issues in power systems," *IEEE Transactions on Power Systems*, vol. 14, no. 1, pp. 3–8, 1999.

[25] F. S. A. Qian, "Application of fast and elitist non-dominated sorting generic algorithm in multi-objective reactive power optimization," *Transactions of China Electrotechnical Society*, vol. 12, p. 24, 2007.

[26] M. Yong-Jie and Y. Wen-Xia, "Research progress of genetic algorithm," *Application Research of Computers*, vol. 29, no. 4, pp. 1201–1206, 2012.

[27] X. Tao, C. Huowang, and Institute of Computer Science, Changsha, China, "Evolutionary algorithms for multi-objective optimization and decision-making problems," *Engineering Science*, vol. 4, no. 2, pp. 1–94, 2002.

[28] K. Deb, A. Pratap, S. Agarwal, and T. Meyarivan, "A fast and elitist multiobjective genetic algorithm: NSGA-II," *IEEE Transactions on Evolutionary Computation*, vol. 6, no. 2, pp. 182–197, 2002.

[29] X. S. Yang and S. Deb, "Cuckoo search via Lévy flights," in *2009 world congress on nature & biologically inspired computing (NaBIC)*, pp. 210–214, Coimbatore, India, 2009.

[30] M. F. Shlesinger, G. M. Zaslavsky, and U. Frisch, "Lévy flights and related topics in physics," *Lecture Notes in Physics*, vol. 450, 1995.